Bull. Korean Chem. Soc. 2013, Vol. 34, No. 7 2183
http://dx.doi.org/10.5012/bkcs.2013.34.7.2183

Notes

NTA-Functionalized Gold Nanoparticles for Visual Detection of Uranyl Ion

Jin Hwan Jung, Se Hwa Jung,[‡] Ji Ha Lee,[†] and Myong Yong Choi[†,*]

Jinjudongmyung High School, Jinju 660-985, Korea
[†]Department of Chemistry and Research Institute of Natural Sciences, Gyeongsang National University, Jinju 660-701, Korea
[*]E-mail: mychoi@gnu.ac.kr
[‡]Jinjujeil Girls' High School, Jinju 660-330, Korea
Received March 23, 2013, Accepted April 2, 2013

Key Words : Chemosensor, Gold Nanoparticles, NTA, Uranyl Ion

Although many metal ions are essential for living cells, their excess accumulation over optimal concentrations in tissues or organs usually consequences various diseases and disorders due to their chelation to essential functional groups, displacement of other metal ions, or involvement in the conformational changes of biologically important molecules.[1-3] Furthermore, heavy transition metals, having radioactive properties such as uranium, cesium, americium, and their isotopes, could impose radiological risks to human. Thus, a development of effective and safe method to remove radionuclides from the body (decorporation) after uranium poisoning is of importance.[2,4-10] The current methods for the removal or recovery of heavy metal ions, such as, ion exchange, chemical precipitation, membrane filtration, and liquid extraction, unfortunately remain unsuitable for the purpose of decorporation.[8] Most of these methods involve expensive and complicated instrumentation, requiring cumbersome laboratory procedures and resulting in low throughput and limited practical application. However, the proposed method in this Note, colorimetric sensing, is of very promising because it needs less labor and inexpensive equipment. Furthermore, its naked-eye detection is much simpler than other closely related methods such as fluorimetric sensors.[11,12]

Nanoparticles modified with noble metals, especially silver and gold, have attracted much attention due to their optical, electrical, and chemical properties.[13-15] In particular, ligand-modified metal nanoparticles have been employed as analytical tools in many environmental and biological fields.[16-18] The surface modification of nanoparticles with appropriate organic ligands not only stabilizes these nanostructures in different solvents, but also provides desirable surface functionalities. Noble metal nanoparticles modified with DNA have generated significant scientific and technological interest.[19] Recently, Mirkin and co-workers reported a DNA-gold nanoparticles-based colorimetric assay, in which the DNA had to be specifically modified for the detection of amino acids and toxic metal ions.[12] Although numerous studies have dealt with the detection of metal ions, there are only a few examples for UO_2^{2+} ion as a chemosensor. Therefore, the study of a chemosensor for UO_2^{2+} ion by using functionalized nanoparticles is still valuable. In this Note, we show that nitrilotriacetic acid-modified gold nanoparticles **1** act as a selective colorimetric probe for UO_2^{2+} ion. Herein, we report the preparation of **1** and its application as a novel colorimetric sensor for UO_2^{2+} ion.

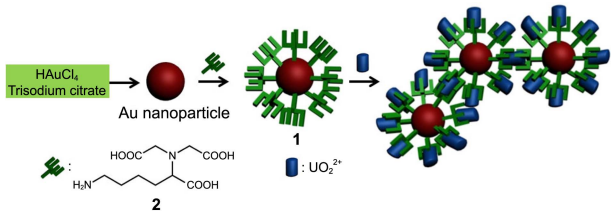

Scheme 1. Schematic illustration of the fabrication of **1** and its aggregation in the presence of UO_2^{2+} in aqueous solution.

The 2,2',2"-nitrilotriacetic acid (NTA) containing aminobutyl group-functionalized gold nanoparticle **1** as a chemosensor for UO_2^{2+} was prepared as shown in Scheme 1. Au nanoparticles were prepared as described previously.[8] The surface of Au nanoparticles was functionalized with NTA **2** at 25 ºC for 2 h. The well-structured carboxyl groups of NTA perform steric effect to shield the Au nanoparticles from agglomeration.[20] Then, the functionalized nanoparticle **1** was well characterized by transmission electron microscopy (TEM), FT-Raman spectroscopy, time-of-flight second ion mass spectroscopy (TOF-SIMS), and UV-Vis spectroscopy.

To verify the immobilization of **2** (Scheme 1) onto the surface of Au nanoparticles, we observed FT-Raman and TOF-SIMS of **1**. Peaks at 3263, 1684, and 1284 cm^{-1} were present in Raman spectrum of **1** (Figure S1). These originated from **2** indicate that **2** was located on the Au nanoparticles. The TOF-SIMS spectrum of **1** displayed the molecular mass for **2** (m/z = 262.26), confirming that **2** was anchored onto the surface of Au nanoparticles (Figure S2). UV-Vis spectrum of free **1** was also observed in aqueous solution at pH 7 (Figure 1). An absorption peak observed at

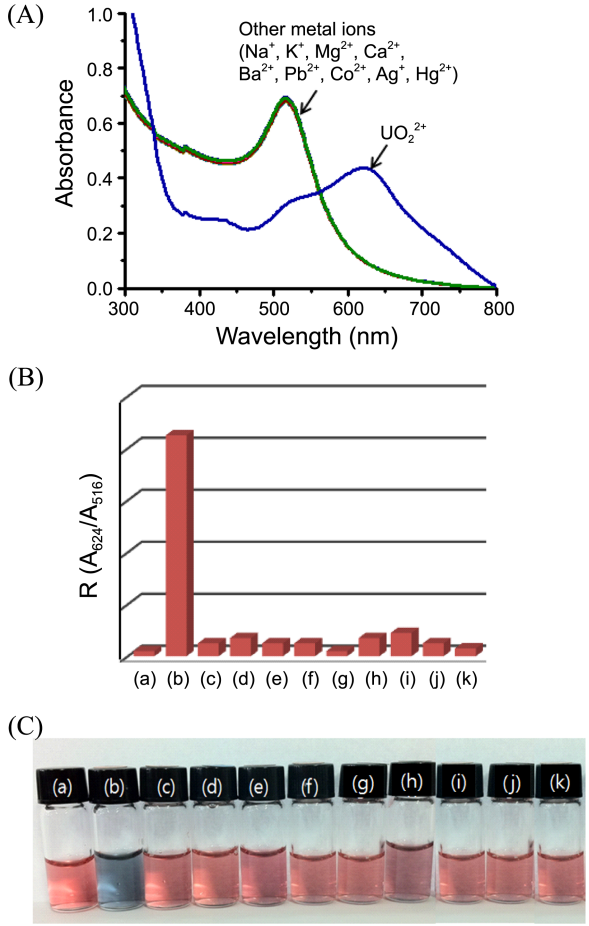

Figure 1. (A) UV-Vis spectra and (B) R (A_{624}/A_{516}) of **1** (10.0 μM) in the presence of metal ions (1.0×10^{-4} M) at pH 7; (a) without metal ion, (b) UO_2^{2+}, (c) Na^+, (d) K^+, (e) Mg^{2+}, (f) Ca^{2+}, (g) Ba^{2+}, (h) Pb^{2+}, (i) Co^{2+}, (j) Ag^+, and (k) Hg^{2+}. (C) Photographic images of **1** containing different amino acids; (a) without metal ion, (b) UO_2^{2+}, (c) Na^+, (d) K^+, (e) Mg^{2+}, (f) Ca^{2+}, (g) Ba^{2+}, (h) Pb^{2+}, (i) Co^{2+}, (j) Ag^+, and (k) Hg^{2+}.

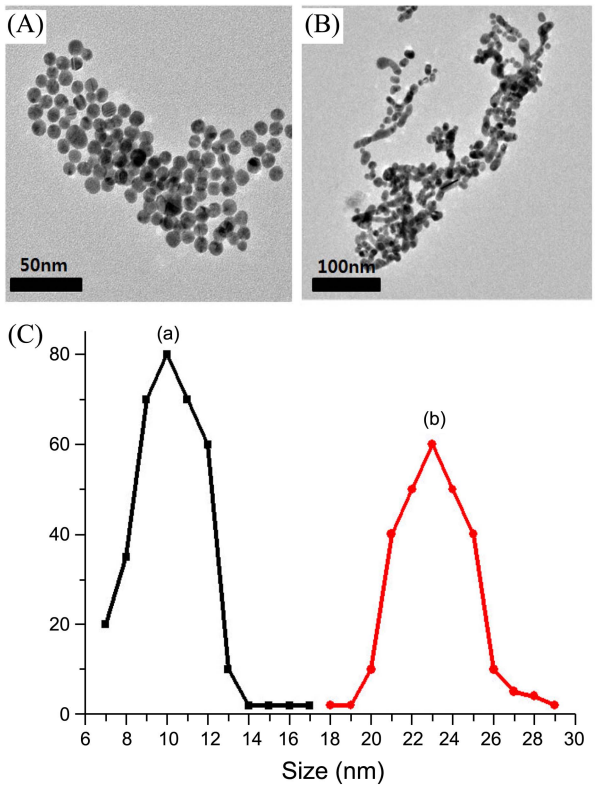

Figure 2. TEM images of **1** (10.0 μM) (A) before and (B) after addition of UO_2^{2+} (1.0×10^{-4} M). (C) The size distribution of **1** (a) before and (b) after addition of UO_2^{2+} in aqueous solution.

516 nm originates from the surface plasmon absorption of **1** without metal ions. The spectrum with a narrow full-width-at-half-maximum (FWHM) indicates that the synthesized Au nanoparticles were monodispersed and uniform.

The color changes of NTA-functionalized Au nanoparticle **1** were observed upon addition of metal ions such as Na^+, K^+, Mg^{2+}, Ca^{2+}, Ba^{2+}, Pb^{2+}, Co^{2+}, Ag^+, Hg^{2+} and UO_2^{2+} in aqueous solution at pH 7. Figure 1(a) illustrates the color changes and R values (A_{624}/A_{516}) of **1** after the addition of solutions (1.0×10^{-4} M) of various metal ions. Over 10 min, the solution containing UO_2^{2+} changed from red to blue, with a dramatic increase in the absorbance ratio A_{624}/A_{516}. The addition of other metal ions, in contrast, had no effect on the color or absorption behavior of **1**. Thus, the sensor **1** responds selectively to UO_2^{2+}, which can be attributed to its aggregation induced by UO_2^{2+}. It is also well-known that the oxygen atoms of UO_2^{2+} can be easily bound to carboxylate anions. Therefore, the UO_2^{2+} ions might be bound to carboxylate of NTA immobilized onto the Au nanoparticles, which induced the aggregation of **1**.

To determine whether the specificity in the detection of UO_2^{2+} is compromised by complex mixtures of other metal ions, we inspected the R values (A_{624}/A_{516}) of **1** with UO_2^{2+} in binary systems (Figure S3). The sensor **1** was added as a stable dispersion in mixtures of these metal ions. However, the color change of **1** from red to blue was observed only

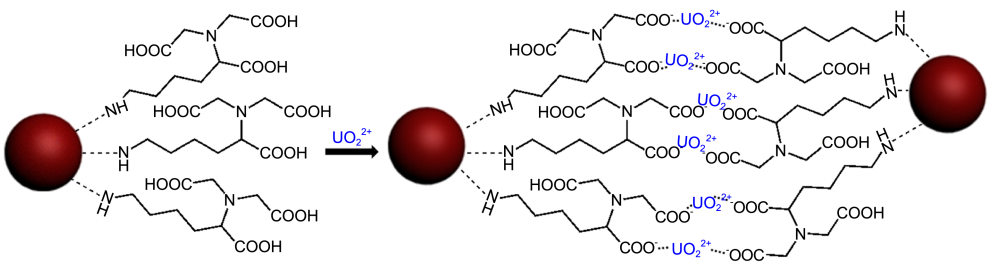

Figure 3. Proposed structure of **1**-UO_2^{2+} complex in aqueous solution.

when a solution of UO_2^{2+} was added to the mixture (Figure 1). Thus, we believe that the highly selective nature of the color change of **1** is due to the high selectivity of the assay for UO_2^{2+}. This result indicates that the detection of UO_2^{2+} can be performed in solution even when a mixture of other metal ions is present.

To investigate the color change of **1** with UO_2^{2+} by comparing their morphologies of **1** and **1** with UO_2^{2+}, we observed the TEM image of **1** before and after addition of UO_2^{2+} (Figures 2(A) and 2(B)). The TEM image shows that prior to the addition of UO_2^{2+}, the particles of **1** are highly dispersed and uniform in aqueous solution with diameters of *ca*. 10 nm. After the addition of UO_2^{2+}, the particles of **1** increased in size and became highly aggregated into aggregates of 20-30 nm of diameter (Figure 2(C)). This aggregation resulted in the red-to-blue color change reflecting to the interparticle coupled plasmon excitons in the aggregated states.

To evaluate the minimum concentration of UO_2^{2+} aqueous solution detectable by the color change, we added UO_2^{2+} into the mixture of **1** over the concentration range 1.0-20.0 μM. UO_2^{2+} was detectable by eye with **1** at levels as low as 1.0 μM (Figure S4). In addition, a linear response between R values (A_{624}/A_{516}) and concentration of **1** was observed between 1.0 and 20.0 μM with a detection limit of *ca*. 1.0 μM.

For a biological or environmental chromogenic sensor, the sensing should be effective over a wide pH range. Thus, we examined the effect of pH on absorbance (A_{624}) of **1** in the presence of UO_2^{2+} (pH 4-12). As shown in Figure S5, the absorbance under neutral and basic conditions was higher than under acidic condition due to the stronger aggregation of **1** with UO_2^{2+} by the electrostatic interaction between the carboxylate anion of **1** and UO_2^{2+} under neutral and basic conditions as shown in Figure 3.

In order to provide direct evidence for the electrostatic interaction between the carboxylate anion of **1** and UO_2^{2+}, we obtained FT-IR spectra of **1** with and without UO_2^{2+}. The vibrational bands for the COO^- species of **1** in the absence of UO_2^{2+} showed strong bands at 1398 and 1386 cm^{-1}. In contrast, in the presence of UO_2^{2+}, the vibrational bands for the COO^- species of **1** showed a strong band at 1404 cm^{-1}. These results are strong evidence for the electrostatic interaction between the UO_2^{2+} and COO^- species of **1**.

In conclusion, we have demonstrated the fabrication of the NTA-functionalized Au nanoparticle **1** and its successful application for the selective visual detection of UO_2^{2+}. We believe that our current approach will provide a more convenient method for selective detection of UO_2^{2+}, when compared with the current methods, which require multi-step processes and expensive instrumentation. We also believe that our approach can be employed for anchoring other target metal ions on nanoparticles, potentially producing a range of novel environmental and biomedical nanomaterials.

Experimental

Instruments. ^1H and ^{13}C NMR spectra were measured with a Bruker 300 apparatus. IR spectra were obtained for KBr pellets, in the range 400-4000 cm^{-1}, with a Shimadzu FT-IR 8400S instrument, and the MS spectrum was obtained with a JEOL JMS-700 mass spectrometer. All UV-Vis absorption spectra were recorded in RF-5301PC spectrophotometer. Time-of-flight second ion mass spectrometer (TOF-SIMS) was analyzed on Model PHI 7200 equipped with Cs and Ga ion guns for positive and negative ion mass detection. FT-Raman spectra were measured by Model LabRAM HR800.

Synthesis of NTA-Modified Gold Nanoparticle (1). Gold nanoparticles with average diameter of *ca*. 20 nm were prepared by the citrate-mediated reduction of $AuCl_3$. An aqueous solution of $AuCl_3$ (5.0 mM, 1.0 mL) was stirred at room temperature, and then sodium citrate solution (30 mM, 1.0 mL), sodium borohydride (50 mM, 1.0 mL) were added quickly, resulting in a change in solution color from pale yellow to deep red. After the color change, the solution was heated under reflux for an additional 30 min and allowed to cool to room temperature. Ligand exchange reactions were performed under stirring at room temperature for 24 h by mixing a given volume of as-prepared gold colloids with water solution containing an excess of 2,2',2"-nitrilotriacetic acid containing aminobutyl group as a functional ligand. The solutions of functionalized gold nanoparticles were centrifuged for 30 min and redispersed in aqueous solution after the supernatant was removed. The particles were washed three more times, and finally redispersed in the detection buffer. The solution was then adjusted to pH 7 by 2-(cyclohexylamino)ethane sulfonic acid (CHES) buffer.

Colorimetric Detection of Metal Ions. For the colorimetric detection of metal ions such as Na^+, K^+, Mg^{2+}, Ca^{2+}, Ba^{2+}, Pb^{2+}, Co^{2+}, Ag^+, Hg^{2+} and UO_2^{2+}, the stock solutions of these metal ions in the detection buffer were mixed with the probe solution prepared as described above at room temperature to a final volume of 1 mL (The final concentration of Au nanoparticles probes was 1.0 μM). The color changes of 1 with 1.0 μM of metal ions were observed. To evaluate the sensitivity of the assay, the final concentrations of UO_2^{2+} were varied from 1.0 to 20.0 μM. The selectivity for UO_2^{2+} was confirmed by the addition of the stock solutions of other metal ions to 1, using the same conditions, with a final metal ion concentration of 20.0 μM.

Acknowledgments. This work was supported by the Korea Ministry of Environment as "GAIA Project" (2012000550026).

Supporting Information. FT-Raman and TOF-SIMS spectrum of **1** nanoparticle, R (A_{624}/A_{516}) of **1** (10.0 μM) in the presence of metal ions (1.0×10^{-4} M) at pH 7, calibration curve of concentration of UO_2^{2+} against absorption intensity of **1** (at 624 nm).

References

1. Gorden, A. E. V.; Xu, J.; Raymond, K. N.; Durbin, P. *Chem. Rev.* **2003**, *103*, 4207.
2. Gutowski, K. E.; Cocalia, V. A.; Griffin, S. T.; Bridges, N. J.;

Dixon, D. A.; Rogers, R. D. *J. Am. Chem. Soc.* **2006**, *129*, 526.
3. Bühl, M.; Diss, R.; Wipff, G. *J. Am. Chem. Soc.* **2005**, *127*, 13506.
4. Franczyk, T. S.; Czerwinski, K. R.; Raymond, K. N. *J. Am. Chem. Soc.* **1992**, *114*, 8138.
5. Sather, A. C.; Berryman, O. B.; Rebek, J. *J. Am. Chem. Soc.* **2010**, *132*, 13572.
6. Kim, K.-C.; Pope, M. T. *J. Am. Chem. Soc.* **1999**, *121*, 8512.
7. Grohol, D.; Clearfield, A. *J. Am. Chem. Soc.* **1997**, *119*, 9301.
8. Wang, L.; Yang, Z.; Gao, J.; Xu, K.; Gu, H.; Zhang, B.; Zhang, X.; Xu, B. *J. Am. Chem. Soc.* **2006**, *128*, 13358.
9. Hayton, T. W.; Boncella, J. M.; Scott, B. L.; Batista, E. R.; Hay, P. J. *J. Am. Chem. Soc.* **2006**, *128*, 10549.
10. Cametti, M.; Nissinen, M.; Dalla Cort, A.; Mandolini, L.; Rissanen, K. *J. Am. Chem. Soc.* **2007**, *129*, 3641.
11. Lee, J.-S.; Lytton-Jean, A. K. R.; Hurst, S. J.; Mirkin, C. A. *Nano Lett.* **2007**, *7*, 2112.
12. Lee, J.-S.; Ulmann, P. A.; Han, M. S.; Mirkin, C. A. *Nano Lett.* **2008**, *8*, 529.
13. Elghanian, R.; Storhoff, J. J.; Mucic, R. C.; Letsinger, R. L.; Mirkin, C. A. *Science* **1997**, *277*, 1078.
14. Lioubashevski, O.; Chegel, V. I.; Patolsky, F.; Katz, E.; Willner, I. *J. Am. Chem. Soc.* **2004**, *126*, 7133.
15. Wessels, J. M.; Nothofer, H.-G.; Ford, W. E.; von Wrochem, F.; Scholz, F.; Vossmeyer, T.; Schroedter, A.; Weller, H.; Yasuda, A. *J. Am. Chem. Soc.* **2004**, *126*, 3349.
16. Durocher, S.; Rezaee, A.; Hamm, C.; Rangan, C.; Mittler, S.; Mutus, B. *J. Am. Chem. Soc.* **2009**, *131*, 2475.
17. Darbha, G. K.; Singh, A. K.; Rai, U. S.; Yu, E.; Yu, H.; Chandra Ray, P. *J. Am. Chem. Soc.* **2008**, *130*, 8038.
18. Stoeva, S. I.; Lee, J.-S.; Smith, J. E.; Rosen, S. T.; Mirkin, C. A. *J. Am. Chem. Soc.* **2006**, *128*, 8378.
19. Braun, G.; Lee, S. J.; Dante, M.; Nguyen, T.-Q.; Moskovits, M.; Reich, N. *J. Am. Chem. Soc.* **2007**, *129*, 6378.
20. Bae, D. R.; Han, W. S.; Lim, J. M.; Kang, S.; Lee, J. Y.; Kang, D.; Jung, J. H. *Langmuir* **2009**, *26*, 2181.